Supplementary Online Content

Priedigkeit N, Hartmaier RJ, Chen Y, et al. Intrinsic subtype switching in breast cancer brain metastases and acquired *ERBB2/HER2* amplifications and activating mutations. *JAMA Oncol*. Published online December 7, 2016. doi:10.1001/jamaoncol.2016.5630.

eTable 1. Clinocopathological features of patient-matched brain metastasis cases.

eTable 2. Multi-gene test clinical classifications in patient-matched pairs.

eFigure 1. Fold change density distribution in patient-matched pairs.

eFigure 2. Recurrent expression alterations (> 1 pair) and most recurrently downregulated and upregulated genes in BrM.

eFigure 3. ER expression loss in breast cancer brain metastases.

eFigure 4. HER2 expression and *ERBB2* copy-number gains in breast cancer brain metastases.

eFigure 5. DNA-level ERBB2 gains in an independent cohort.

This supplementary material has been provided by the authors to give readers additional information about their work.

SUPPLEMENTAL ONLINE CONTENT

Breast cancer brain metastases show limited intrinsic subtype switching, yet exhibit acquired *ERBB2* amplifications and activating mutations.

JAMA Oncology Brief Report Manuscript Submission

Supplemental Methods

eTable 1. Clinocopathological features of patient-matched brain metastasis cases.

eTable 2. Multi-gene test clinical classifications in patient-matched pairs.

eFigure 1. Fold change density distribution in patient-matched pairs.

eFigure 2. Recurrent expression alterations (> 1 pair) and most recurrently downregulated and upregulated genes in BrM.

eFigure 3. ER expression loss in breast cancer brain metastases.

eFigure 4. HER2 expression and *ERBB2* copy-number gains in breast cancer brain metastases.

eFigure 5. DNA-level ERBB2 gains in an independent cohort.

Supplemental References

SUPPLEMENTAL METHODS

Patient enrollment. In total, 20 cases of patient-matched primary breast tumors (10 ER-, 10 ER+) and BrM from two institutions were included—6 pairs from Royal College of Surgeons (RCS), Ireland and 14 pairs from University of Pittsburgh (Pitt), USA (eTable 1). This study was reviewed and approved by Institutional Review Boards from both participating institutions (University of Pittsburgh IRB# PRO15050502, Royal College of Surgeons IRB #09-07). An independent, controlled-access dataset of 17 patient-matched samples with brain metastases generated by the Broad Institute was acquired from dbGap (phs000730.v1.p)[1] under the IRB# PRO16030233. A collection of 7,884 breast cancer tumor data (52% metastases, including BrM) was analyzed from Foundation Medicine with study approval by the Western Institutional Review Board (WIRB).

Tissue Processing. Formalin-fixed paraffin-embedded (FFPE) tumor blocks were sectioned and H&E staining analyzed by a pathologist (PCL) for histological and tumor cellularity classifications. All specimens had a tumor cellularity equal to or above 60% except for BM_Pitt_68 (40%) and BM_Pitt_71 (30%). Between four to ten (depending on tumor size) 10-micron FFPE sections immediately adjacent to the H&E-analyzed section were scrolled and pooled for dual DNA/RNA extraction using Qiagen's AllPrep kit according to manufacturer's instructions.

NanoString and RNA expression. Samples were analyzed using a NanoString codeset consisting of probes for 141 genes (127 target, 14 housekeeping) as previously reported (Data Supplement S1)[2].

Clustering and Molecular Subtyping. Hierarchical clustering was performed on normalized expression data (Data Supplement S2, S3). Clustering was performed using the hclust function in R, with 1 minus Pearson correlation as distance measures and the "average" agglomeration method. Heatmap was created with heatmap.3 in R. PAM50 molecular subtyping was performed using genefu[3]. To account for PAM50 test set bias[4], normalized expression data from a cohort of 20 tumor samples with known ER-status were subsampled to create a balanced cohort of ER-positive and ER-negative tumors. A query sample of unknown molecular subtype was added to the balanced cohort. Expression data was then median centered and an intrinsic molecular subtype was called for the query sample using the pam50.robust model in genefu. This method was repeated for all 40 clinical specimens (Data Supplement S4). OncoTypeDX scores were determined using unscaled genefu OncoTypeDX scores and a linear model generated from 72 samples with known OncoTypeDX scores as performed previously[2].

Recurrent expression alterations and clinically actionable genes. An 'expression alteration' was defined as a 2-fold change in normalized expression counts (Data Supplement S5). This threshold was chosen because the mean log2 fold-change between primary and metastatic lesions for all genes across all samples was -0.01 with a standard deviation of 1.04 (i.e. approximately a 2-fold change). Recurrent alterations were plotted using *ComplexHeatmap*[5]. To interrogate clinically significant alterations, the Drug-Gene Interaction (DGIdb 2.0) database was used[6]. All genes were input into the database and only those annotated as 'clinically actionable' (as of March 10th, 2016) were visualized.

To plot and statistically assess gene-specific expression differences, the *beeswarm R* package was used to create ladder plots along with Wilcoxon signed-rank tests on paired (primary vs. metastasis) normalized log2 expression values.

IHC Staining. 10 micron FFPE sections were mounted on slides and stained for HER2 and ER as described previously[7].

Copy number variation (CNV) and Single Nucleotide Variant (SNV) Analysis. Tumor DNA quality was assessed by an Illumina FFPE QC Kit. DNA with a Delta Cq value below 5 were restored using the Infinium HD FFPE DNA Restore Kit. 200 ng of restored tumor DNA was ran on an Illumina iScan System using an Illumina HumanCytoSNP-FFPE v.2.1 BeadChip. GenomeStudio was implemented to produce normalized logR intensity values from the two-color readouts using the HumanCytoSNP-12v2.1-FFPE_G.egt cluster file. These values were then analyzed using the *copynumber* package in R[8]. LogR values were preprocessed by excluding outliers via Winsorization and imputing missing measurements as a logR value of 0. Data then underwent multi-sample segmentation and final LogR values and segments were assessed and plotted for chromosome 17 (Data Supplement S6). Raw fastq files from whole-exome sequencing of an independent cohort of 17 patient-matched primary BrCa and BrM were aligned using bwa (v0.7.13), sorted with samtools (v1.3), duplicates marked and removed with picardtools (v1.140) and local realignment performed with GATK (v3.4-46) [9-11]. To estimate and plot logR ratios, CNVkit was utilized on processed bam files[12]. A pool of bam files from normal tissue was used as a CNVkit reference. Log2 ratio estimates were then analyzed for metastasis-specific gains in ERBB2 by performing a student's t-test on primary and metastatic estimated logR values across the 26 ERBB2 exonic regions (Data Supplement S7). To discover ERBB2 activating mutations in the HER2-switching PB0049 case, the ERBB2 region was probed for somatic mutations using CLC Genomics Workbench (http://www.clcbio.com, v9.0) and IGV (v2.3.60)[13].

FoundationOne ERBB2 Alterations. To test whether ERBB2 amplification and base pair mutation is metastasis-site specific, changes in this gene were evaluated in an expanded cohort of 7,884 breast tumors enriched for metastatic samples (52%) including liver (16.7%), lung (4.3%), bone (3.6%), and brain (2.0%) that underwent genomic profiling as part of routine clinical care in a CLIA-certified, CAP-accredited, and New York State-accredited laboratory[14]. ERBB2 alterations were identified as described previously[14,15]. ERBB2 alteration types and frequencies in local breast cancer tumors and brain metastasis can be found in Data Supplement S8.

eTable 1. Clinocopathological features of patient-matched brain metastasis cases.

Case	Tissue Source	Pathology	ER Status	PR Status	Her2 Status	Endocrine Therapy	HER2 Therapy
RCS_1	RCS	IDC	Neg	Neg	Pos	-	-
RCS_2	RCS	IDC	Neg	Neg	Pos	-	+
RCS_3	RCS	IDC	Pos	Neg	Pos	NA	+
RCS_4	RCS	IDC	Pos	Neg	Neg	+	-
RCS_5	RCS	IDC	Neg	Neg	Neg	-	-
RCS_6	RCS	IDC	Pos	Neg	Neg	+	-
Pitt_6	Pitt	IDC	Neg	Neg	Neg	-	-
Pitt_7	Pitt	IDC	Pos	Neg	Pos	+	+
Pitt_12	Pitt	IDC	Neg	Neg	Neg	-	-
Pitt_17	Pitt	IDC	Pos	Neg	Pos	-	+
Pitt_25	Pitt	IDC	Neg	Neg	Neg	-	-
Pitt_29	Pitt	IDC	Pos	Neg	Neg	-	-
Pitt_47	Pitt	IDC/ILC	Pos	Pos	Pos	+	+
Pitt_51	Pitt	IDC	Pos	Neg	Neg	+	-
Pitt_52	Pitt	IDC	Neg	Pos	Pos	-	+
Pitt_62	Pitt	IDC	Pos	Pos	Neg	+	NA
Pitt_64	Pitt	IDC	Neg	Neg	Neg	-	-
Pitt_68	Pitt	IDC	Neg	Neg	Neg	+	-
Pitt_71	Pitt	IDC	Neg	Neg	Neg	-	-
Pitt_72	Pitt	ILC	Pos	Pos	Neg	+	-

Abbreviations: ER, estrogen receptor; PR, progesterone receptor; HER2, human epidermal growth factor receptor 2; IDC, invasive ductal carcinoma; ILC, invasive

lobular carcinoma. Hormone receptor status were called from IHC as per ASCO/CAP recommendations[16,17].

eTable 2. Multi-gene test classifications in patient-matched pairs

Case	PAM50 Subtype	OncoTypeDX Score	OncoTypeDX Risk
BP_RCS_1	Her2	41.2	1
BM_RCS_1	Her2	55.2	1
BP_RCS_2	LumA	15.6	0
BM_RCS_2	Her2*	60.9	1*
BP_RCS_3	LumB	40.2	1
BM_RCS_3	LumB	56.4	1
BP_RCS_4	LumB	9.8	0
BM_RCS_4	LumA*	3.3	0
BP_RCS_5	Basal	58.6	1
BM_RCS_5	Basal	66.3	1
BP_RCS_6	LumA	-4.9	0
BM_RCS_6	LumA	12.6	0
BP_Pitt_6	Basal	29.9	0.5
BM_Pitt_6	Basal	12.8	0*
BP_Pitt_7	Her2	55.1	1
BM_Pitt_7	Her2	60.0	1
BP_Pitt_12	Basal	32.1	1
BM_Pitt_12	Basal	52.3	1
BP_Pitt_17	LumA	7.5	0
BM_Pitt_17	LumA	25.1	0.5*
BP_Pitt_25	Basal	50.0	1
BM_Pitt_25	Basal	36.9	1
BP_Pitt_29	Basal	66.5	1
BM_Pitt_29	Basal	59.0	1
BP_Pitt_47	LumA	-9.3	0
BM_Pitt_47	Her2*	13.8	0
BP_Pitt_51	LumB	33.5	1
BM_Pitt_51	LumB	28.9	0.5*
BP_Pitt_52	Her2	39.5	1
BM_Pitt_52	Her2	39.4	1
BP_Pitt_62	LumB	14.6	0
BM_Pitt_62	LumB	31.4	1*
BP_Pitt_64	Basal	51.5	1
BM_Pitt_64	Basal	46.5	1
BP_Pitt_68	Basal	53.0	1
BM_Pitt_68	Basal	45.2	1
BP_Pitt_71	Basal	48.9	1
BM_Pitt_71	Basal	53.5	1
BP_Pitt_72	LumA	-2.3	0
BM_Pitt_72	LumA	0.1	0

Case along with PAM50 subtype calls, inferred OncoTypeDX score and corresponding

clinical risk value. Discordant pairs are marked with an asterisks.

eFigure 1. Fold change density distribution in patient-matched pairs.

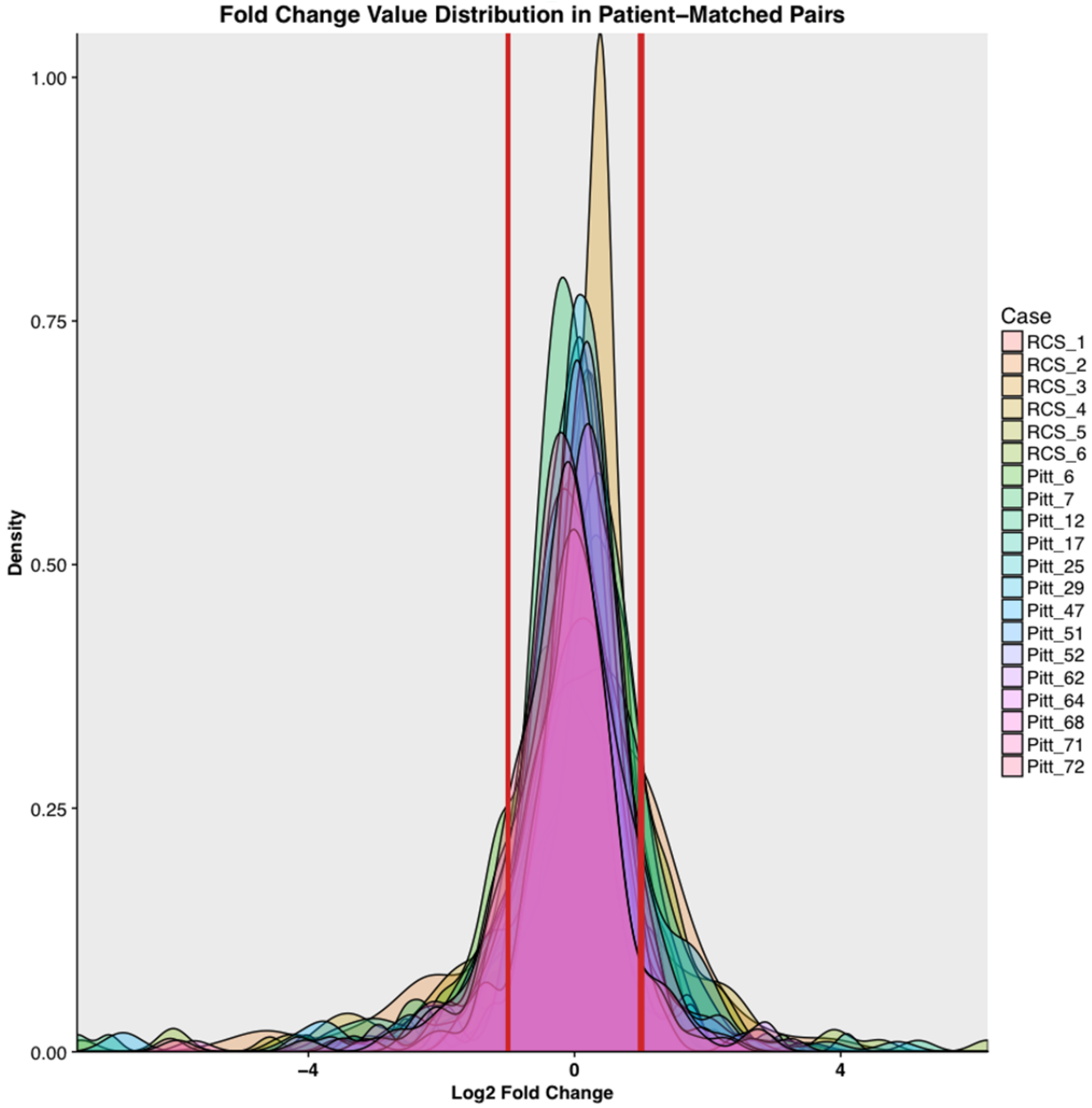

Fold-change value density plot for each case (i.e. Log2 brain metastasis normalized expression – Log2 primary metastasis normalized expression). Mean is -0.01 and 1 standard deviation above and below the mean are marked with vertical red lines. Expression alterations outside these lines were counted as 'expression alterations'.

eFigure 2. Recurrent expression alterations (> 1 pair) in breast cancer brain metastases and most recurrently downregulated and upregulated genes in BrM.

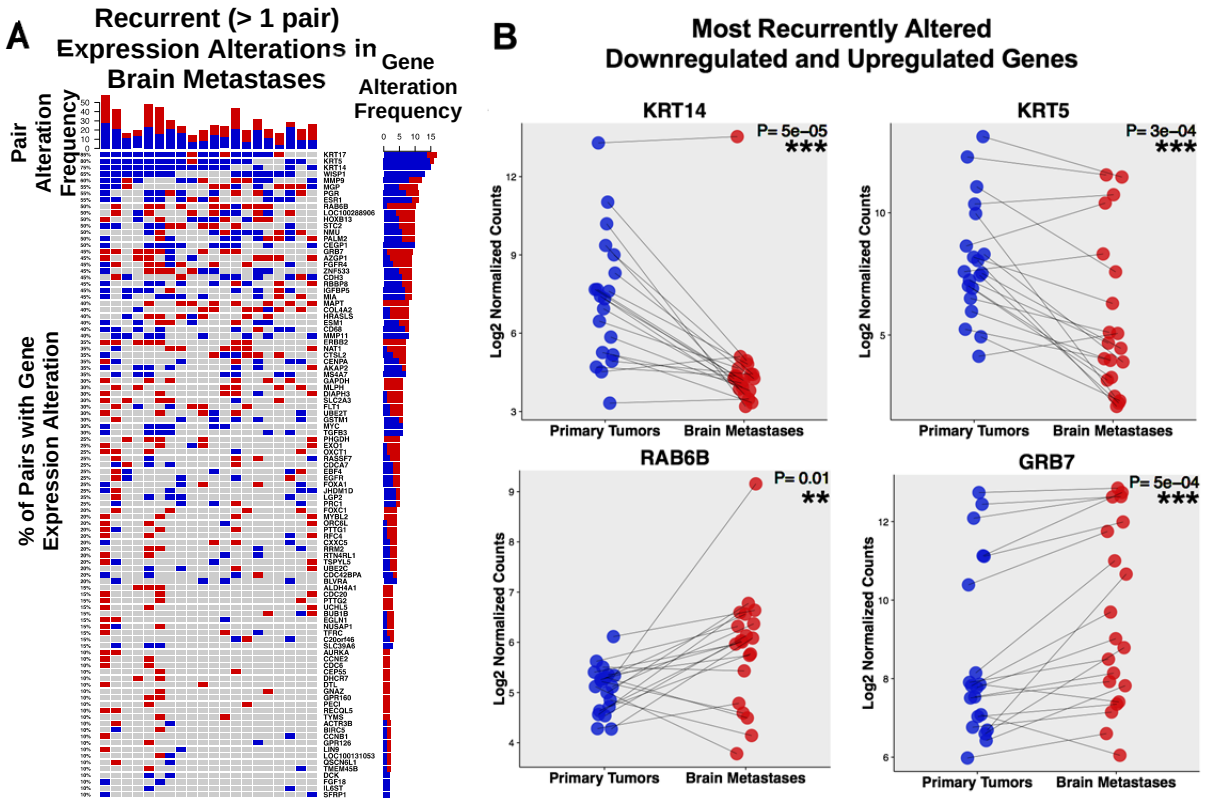

(A) OncoPrint plot of all recurrent (altered in > 1 case) expression alterations in 20 cases, ranked by frequency of alteration by gene. Blue tile represents a >2-fold decrease in the patient-matched brain metastasis relative to the primary, while a red tile represents a >2-fold increase. **(B)** Paired ladder plots visualizing case-specific alterations in the most recurrently upregulated and downregulated genes interrogated. Blue dots represent primary tumor expression values (Log2 normalized counts), red dots represent metastatic tumor expression values; p-values (* p <= 0.05, ** p <= 0.01, *** p <= 0.001) shown are from Wilcoxon signed-rank tests (primaries vs. metastases).

eFigure 3. ER expression loss in breast cancer brain metastases.

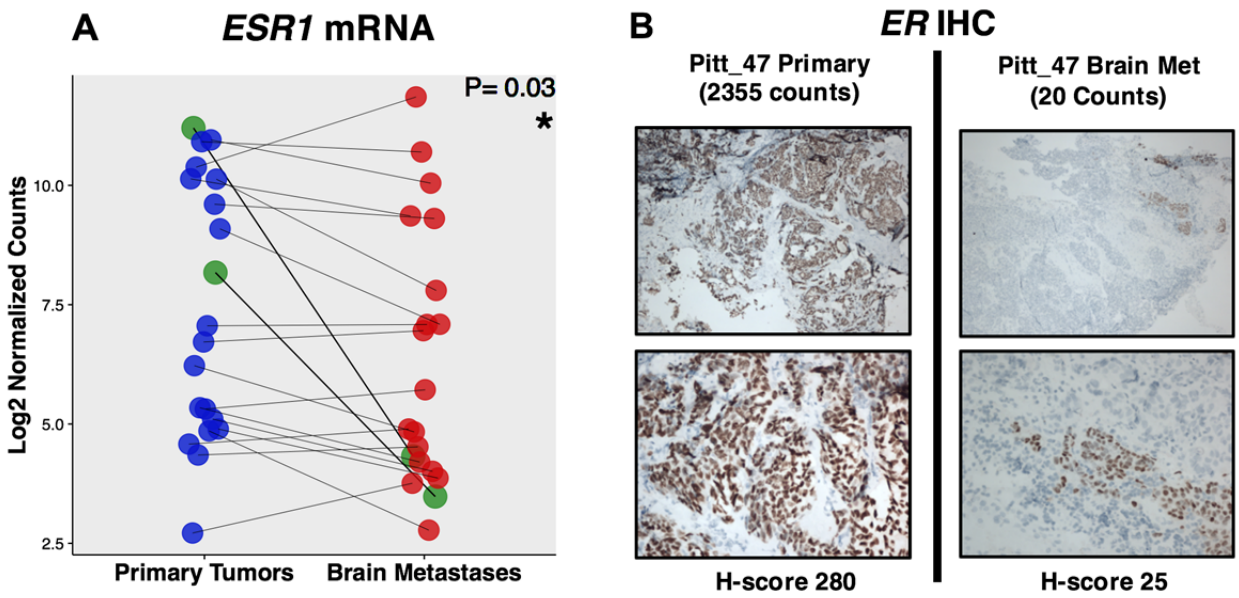

(A) Paired ladder plot of *ESR1* expression in patient-matched cases. Green dots represent samples with suspected hormone status switching, p-values (* p <= 0.05, ** p <= 0.01, *** p <= 0.001) shown are from Wilcoxon signed-rank tests (primaries vs. metastases). **(B)** Primary and metastatic IHC staining of ER from case Pitt_47, along with normalized NanoString expression counts and pathological H-score. Top images are low magnification, bottom images are high magnification.

eFigure 4. HER2 expression and *ERBB2* copy-number gains in breast cancer brain metastases.

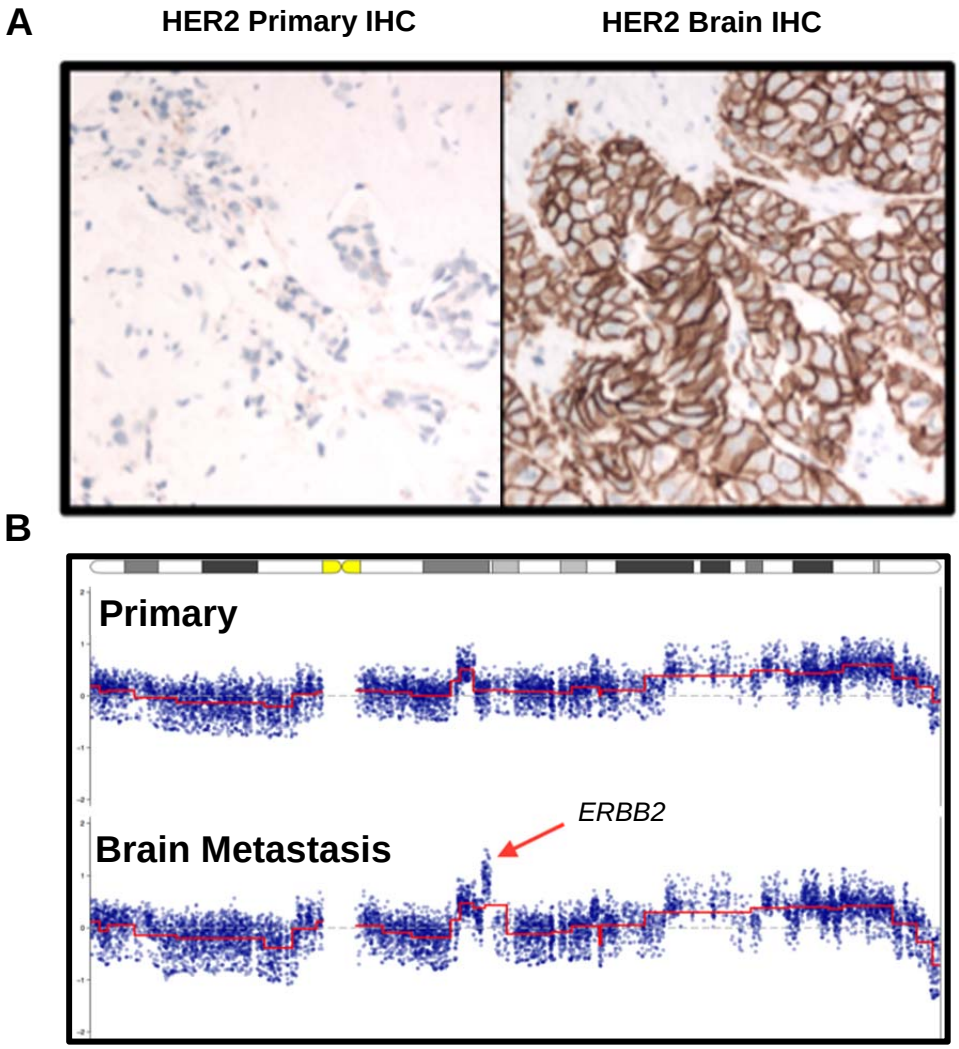

(A) Primary and Metastatic IHC staining of HER2 from case Pitt_62. **(B)** LogR value plot for chromosome 17 in primary and brain metastasis from case Pitt_62. ERBB2 region highlighted with a red arrow.

eFigure 5. DNA-level ERBB2 gains in an independent cohort.

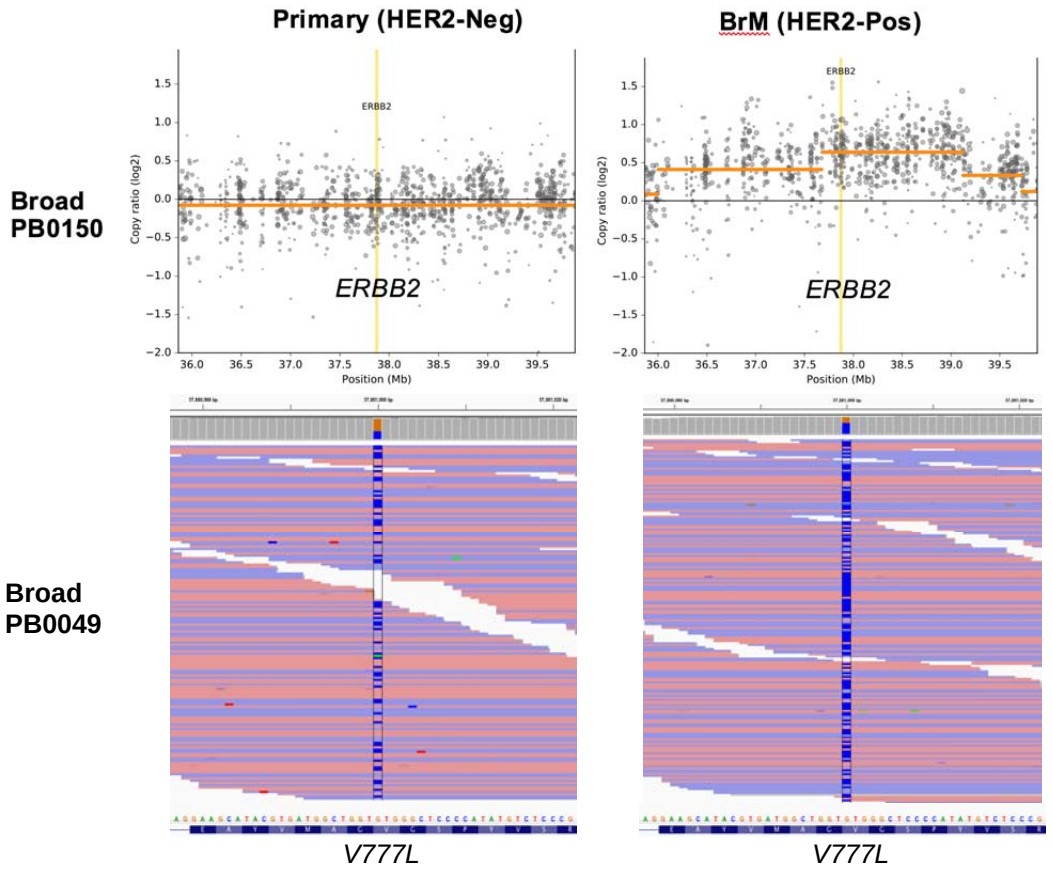

Top; Broad PB0150 *CNVkit* LogR plots from primary and brain metastasis. Segmented LogR ratio means are marked with horizontal orange lines across a 4 MB region surrounding the *ERBB2* locus (designated with a vertical yellow line). Bottom; PB0049 V777L activating *ERBB2* mutation in primary and brain metastasis as visualized in IGV. G to C variant highlighted in blue, along with variant frequency barplots above.

SUPPLEMENTAL REFERENCES

1. Brastianos PK, Carter SL, Santagata S, et al. Genomic Characterization of Brain Metastases Reveals Branched Evolution and Potential Therapeutic Targets. *Cancer Discovery*. 2015;5(11):1164-1177. doi:10.1158/2159-8290.CD-15-0369.

2. Gyanchandani R, Lin Y, Lin H-M, et al. Intra-tumor heterogeneity affects gene expression profile test prognostic risk stratification in early breast cancer. *Clin Cancer Res*. May 2016:clincanres.2889.2015. doi:10.1158/1078-0432.CCR-15-2889.

3. Gendoo DMA, Ratanasirigulchai N, Schröder MS, et al. Genefu: an R/Bioconductor package for computation of gene expression-based signatures in breast cancer. *Bioinformatics*. November 2015:btv693. doi:10.1093/bioinformatics/btv693.

4. Patil P, Bachant-Winner P-O, Haibe-Kains B, Leek JT. Test set bias affects reproducibility of gene signatures. *Bioinformatics*. 2015;31(14):2318-2323. doi:10.1093/bioinformatics/btv157.

5. Gu Z, Eils R, Schlesner M. Complex heatmaps reveal patterns and correlations in multidimensional genomic data. *Bioinformatics*. May 2016:btw313. doi:10.1093/bioinformatics/btw313.

6. Wagner AH, Coffman AC, Ainscough BJ, et al. DGIdb 2.0: mining clinically relevant drug-gene interactions. *Nucleic Acids Res*. 2016;44(D1):D1036-D1044. doi:10.1093/nar/gkv1165.

7. Gloyeske NC, Woodard AH, Elishaev E, et al. Immunohistochemical profile of breast cancer with respect to estrogen receptor and HER2 status. *Appl Immunohistochem Mol Morphol*. 2015;23(3):202-208. doi:10.1097/PAI.0000000000000076.

8. Nilsen G, Liestøl K, Van Loo P, et al. Copynumber: Efficient algorithms for single- and multi-track copy number segmentation. *BMC Genomics*. 2012;13(1):591. doi:10.1186/1471-2164-13-591.

9. Li H, Durbin R. Fast and accurate short read alignment with Burrows-Wheeler transform. *Bioinformatics*. 2009;25(14):1754-1760. doi:10.1093/bioinformatics/btp324.

10. Li H, Handsaker B, Wysoker A, et al. The Sequence Alignment/Map format and SAMtools. *Bioinformatics*. 2009;25(16):2078-2079. doi:10.1093/bioinformatics/btp352.

11. McKenna A, Hanna M, Banks E, et al. The Genome Analysis Toolkit: a MapReduce framework for analyzing next-generation DNA sequencing data. *Genome Res*. 2010;20(9):1297-1303. doi:10.1101/gr.107524.110.

12. Talevich E, Shain AH, Botton T, Bastian BC. CNVkit: Genome-Wide Copy Number Detection and Visualization from Targeted DNA Sequencing. *PLoS Comput Biol*. 2016;12(4):e1004873. doi:10.1371/journal.pcbi.1004873.

13. Robinson JT, Thorvaldsdottir H, Winckler W, et al. Integrative genomics viewer. *Nature Biotechnology*. 2011;29(1):24-26. doi:10.1038/nbt.1754.

14. Frampton GM, Fichtenholtz A, Otto GA, et al. Development and validation of a clinical cancer genomic profiling test based on massively parallel DNA sequencing. *Nature Biotechnology*. 2013;31(11):1023-1031. doi:10.1038/nbt.2696.

15. Chmielecki J, Ross JS, Wang K, et al. Oncogenic alterations in ERBB2/HER2 represent potential therapeutic targets across tumors from diverse anatomic sites of origin. *Oncologist*. 2015;20(1):7-12. doi:10.1634/theoncologist.2014-0234.

16. Hammond MEH, Hayes DF, Dowsett M, et al. American Society of Clinical Oncology/College Of American Pathologists guideline recommendations for immunohistochemical testing of estrogen and progesterone receptors in breast cancer. *Journal of Clinical Oncology*. 2010;28(16):2784-2795. doi:10.1200/JCO.2009.25.6529.

17. Wolff AC, Hammond MEH, Hicks DG, et al. Recommendations for human epidermal growth factor receptor 2 testing in breast cancer: American Society of Clinical Oncology/College of American Pathologists clinical practice guideline update. *Journal of Clinical Oncology*. 2013;31(31):3997-4013. doi:10.1200/JCO.2013.50.9984.